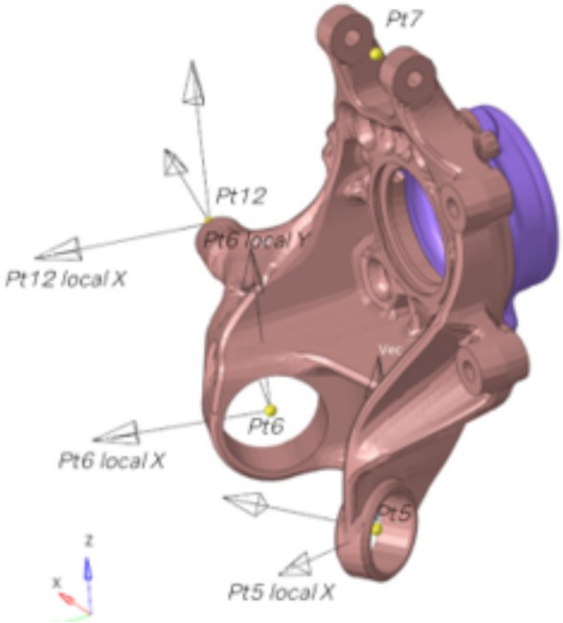

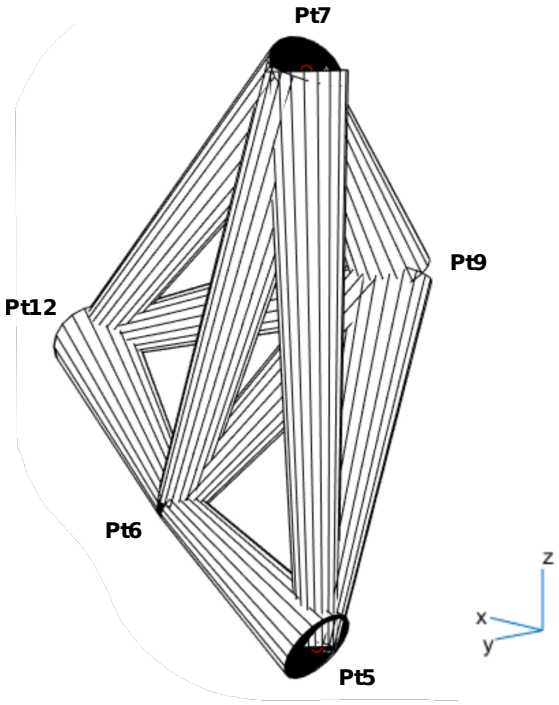

Generic Knuckle Concept Model for Wheel Suspension Performance

Master's thesis in Applied Mechanics

EZHILAN KUMAR

DEPARTMENT OF MECHANICS AND MARITIME SCIENCE

CHALMERS UNIVERSITY OF TECHNOLOGY
Gothenburg, Sweden 2024
www.chalmers.se

Master's thesis 2024

Generic Knuckle Concept Model for Wheel Suspension Performance

EZHILAN KUMAR

CHALMERS
UNIVERSITY OF TECHNOLOGY

Department of Mechanics and Maritime Science
Division of Dynamics
Chalmers University of Technology
Gothenburg, Sweden 2024

Generic Knuckle Concept Model for Wheel Suspension Performance
EZHILAN KUMAR

Examiner and Academic Supervisor:
Petri Piiroinen
Director of Studies
Department of Mechanics and Maritime Sciences
Chalmers University of Technology

Industrial Supervisor:
Akshay Naik
Suspension Architecture
Wheel Suspension, Volvo Car Corporation

Master's Thesis 2024
Department of Mechanics and Maritime Sciences
Division of Dynamics
Chalmers University of Technology
SE-412 96 Gothenburg
Telephone +46 31 772 1000

Cover: ADAMS Car model of the rear right suspension system and the frame structure from the mathematical model.

Typeset in LaTeX
Printed by Chalmers Reproservice
Gothenburg, Sweden 2024

Generic Knuckle Concept Model for Wheel Suspension Performance
EZHILAN KUMAR
Department of Mechanics and Maritime Sciences
Chalmers University of Technology

Abstract

The knuckle is a wheel suspension component that transfers the forces acting upon the tires through the linkages to the vehicle's sub-frame. The coordinates, or joints, where the knuckle and linkages connect are the outer hardpoints and the joints where the linkages and vehicle's sub-frame connect are the inner hardpoints. The position of hardpoints in 3D space will determine the motion of the wheels during different maneuvers.

In the concept phase of the suspension system development, the hardpoints are computed and analyzed iteratively for optimum kinematics and compliance behavior. The suspension knuckle is developed based on the hardpoints. However, optimizing the knuckle design based on stiffness and weight targets for different test cases is time-consuming. Therefore, a quick computation of the knuckle's approximate stiffness right after the iteration of hardpoints in the concept phase will speed up the suspension development process.

This quick approximation of the stiffness, using the concept of 3D-frame analysis, is computed using the Direct Stiffness Method. The frame structure is formed by joining the outer hardpoints using 3D beam elements of uniform and linearly varying cross-sections. The four-link suspension system is mathematically modeled to compute the reaction forces at the outer hardpoints for the applied force at the tire contact patch. The deformation of the nodes at each knuckle hardpoint is calculated based on the reaction forces and appropriate constraints. This mathematical model is validated using NX Finite Element software using 1D elements of uniform and varying cross-sections. Upon validation, the mathematical model is compared against the finite element model of the knuckle for camber and aligning torque stiffness.

Keywords: Non-prismatic 3D beam, four-link suspension, knuckle compliance, frame structure.

Acknowledgements

This master's thesis was conducted at Volvo Cars Corporation, Gothenburg, Sweden. I would like to express my sincere gratitude to Tobias Brandin, Akshay Naik, and Jenny Berglund for providing me with the opportunity to work on this thesis and for their invaluable guidance and support throughout the project.

I would also like to extend my heartfelt thanks to my examiner at Chalmers University of Technology, Petri Piiroinen, for his insightful feedback and continuous encouragement, which greatly contributed to the success of this thesis.

Additionally, I am grateful to Martin Ceballos and Lilly Ma for their assistance in providing the necessary data, which was crucial for comparing and validating my results.

Thank you to everyone who supported me during this journey. Your contributions and encouragement have been instrumental in the completion of this work.

Ezhilan Kumar, Gothenburg, June 2024

Nomenclature

Symbols

A	Area of a cross-section of the beam element $[m^2]$
d_{i-j}	Distance between hardpoints i and j $[m]$
d_1, d_2	Start and end diameters of the element respectively $[m]$
E	Young's modulus $[\frac{N}{m^2}]$
f	Flexibility matrix
G	Shear modulus $[\frac{N}{m^2}]$
I_y, I_z	Second moments of inertia $[m^4]$
J	Polar moment of inertia $[m^4]$
K	Global stiffness matrix of the whole structure
K^e_{local}	Element stiffness matrix in its local coordinates
K^e_{global}	Element stiffness matrix in its global coordinates
L	Length of the element $[m]$
M_{cp}	Moment at Pt6 due to the forces at the wheel contact point $[\frac{N}{m}]$
r	Radius of the beam element $[m]$
T	Transformation matrix
ϕ, θ , ψ	Euler angles of rotation about x, y, and z-axes respectively

Abbreviations

1D, 3D	1 and 3-Dimension respectively
CAD	Computer Aided Designing
CAE	Computer Aided Engineering
CP	Wheel contact point
DOF	Degrees of Freedom
FE	Finite Element
NVH	Noise, Vibration and Harshness

Contents

List of Figures

List of Tables

1

Introduction

1.1 Background and Problem Description

The process of wheel suspension development is complex since many factors need to be considered to ensure that all performance and packaging requirements are met. Wheel suspension tuning must be carried out to meet the vehicle handling, ride comfort, Noise, Vibration, and Harshness (NVH), and durability attribute targets. This requires CAD modeling, multi-body simulations of kinematics, elasto-kinematics, and component flex behaviors for different load cases, which is a rather time-consuming process with many manual steps and various software. To improve efficiency and accuracy in the early concept phase, there is a need to capture kinematic and structural compliance behaviors to define the stiffness targets for the suspension even before CAD models are available.

The usual workflow in the wheel suspension design begins with the generation of hardpoint coordinates in 3D space. It is then used to develop a CAD model of the knuckle and followed by the Finite Element (FE) analysis of the knuckle to test for its compliance. This whole process repeats until all the aforementioned requirements are met. Developing a mathematical model that approximates the stiffness of the knuckle, based on the hardpoint coordinates, will help the engineers decide on the coordinates before having the knuckle's CAD model.

1.2 Objectives

This thesis aims to find a method to develop a mathematical model that aids wheel suspension design engineers in deciding whether the knuckle created with a certain set of hardpoints will meet the optimum stiffness targets set by the CAE engineers. The hardpoints will be developed based on iterations. There is a need to quickly identify the knuckle's corresponding stiffness values to help decide the hardpoint locations even before the CAD model of the knuckle is available.

The idea is to develop a mathematical model of the knuckle in the form of a frame structure. This knuckle structure is formed by joining the hardpoint coordinates on the knuckle side of the suspension system using 3D frame elements. The element properties such as material and cross-sections, and the number of elements to form the frame structure are to be chosen such that the mathematical model approximates the stiffness results from the FE knuckle model.

1.3 Limitations

This thesis focuses primarily on developing a conceptual mathematical model for a rear knuckle, which inherently may not achieve the same level of accuracy as a detailed FE analysis. However, the objective is to provide a tool that aids in the early concept phase of suspension design. As long as the results from the mathematical model fall within an acceptable range of deviation, typically within 25% of the FE model's results, they are deemed adequate for initial design decisions.

It is important to note that this thesis does not aim to enhance or optimize the FE analysis process of the knuckle itself. The scope is limited to mathematically modeling the knuckle using 3D beam elements to assess the model's camber and aligning torque stiffness. Other components integral to the suspension system, such as tires, linkages, and bushings are not included in this mathematical model. The mathematical model will be done for the four-link suspension system of the vehicle, and its wire-frame model is illustrated in Figure 2.2.

For the implementation of the mathematical model, MATLAB will be utilized due to its capabilities in numerical computing and modeling. Concurrently, Siemens NX will be employed for FE analysis of the frame structure, while ADAMS Car will facilitate static multi-body simulations to validate the reaction forces at the outer hardpoints. The results from the mathematical model, upon validation from Siemens NX, will be compared with those provided by the Volvo Car Corporation.

1.4 Methodology

The thesis work was carried out in the following methods:

- Literature survey
  - Understand how knuckles are analyzed for compliance within the organization.
  - Review research papers and books to develop the mathematical model of the knuckle.
- Benchmark study of existing wheel suspension knuckles to establish reference models for front and rear axles.
  - Get to know how the front and rear knuckles differ from each other, and from one car to another.
  - Obtain a reference model to develop the mathematical model.
- Build a simplified conceptual mathematical model to capture the structural compliance.
  - Develop a 1-D mathematical model for a frame structure that outputs the displacements of the structure for prescribed forces and constraints.
- Use the model to identify realistic knuckle stiffness requirements and weight targets.

  - Use the prescribed forces and constraints used by the CAE team which is responsible for compliance study on the knuckle.
  - Develop the model such that it can identify the knuckle's stiffness and weight for a set of suspension hardpoints.
- Verify the accuracy of the conceptual model from commercially built software for different load cases.
  - Compare the results with FE analysis and identify the error percentages for stiffness and weight.
- Prepare the requirements to guide the future knuckle design.
  - Create instructions/guide on the requirements and how the future knuckle designs can be carried out in the organization using this thesis.

2

Theory

The rear knuckle with a four-link suspension system is considered in this thesis. This section intends to describe the theory used to develop the mathematical model to approximate the stiffness of the knuckle for different load cases.

2.1 Knuckle

The knuckle is a wheel suspension component that transfers the forces acting upon the tires through the linkages to the vehicle's sub-frame. At the front wheels, the knuckle can rotate around the steering axis to steer or turn the wheel, facilitated by the force from the steering link connected to the steering rack. At the rear, the knuckle is equipped with a toe-link instead of a steering link, maintaining the rear wheel's toe-setting rather than steering. During driving, the knuckle experiences deformation or compliance due to the forces acting on it, which may result in undesired kinematic characteristics. To mitigate these effects, it is necessary to keep the compliance of the knuckle within a certain range.

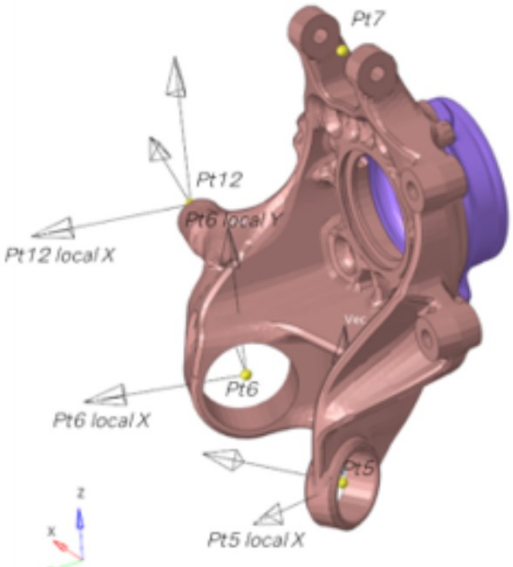

Figure 2.1: CAD model of the rear knuckle.

The reaction forces at the outer hardpoints are considered as prescribed forces, and the corresponding displacement is calculated using the global stiffness matrix constructed for a particular frame structure to approximate the knuckle's stiffness.

2.2 Four-Link Suspension System

The four-link suspension system is similar to the double-wishbone system, except that the lower control arm is split into two-point links in the former. The links are assumed to be rigid, along with the spring, to calculate the reaction forces at the outer hardpoints.

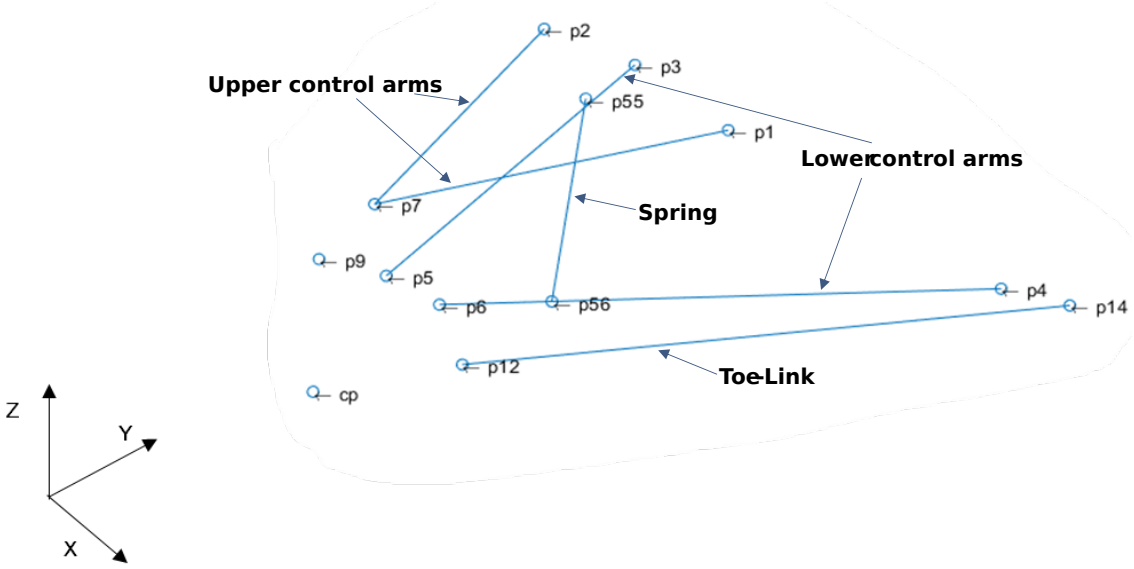

Figure 2.2: The wireframe model of the four-link suspension system.

Figure 2.2 represents the rear left wireframe model of the four-link system. The line joining points p2 and p7, and p1 and p7 represent the upper control arm. The lines joining points p3 and p5, and p4 and p6 define the lower control arm. The line joining p14 and p12 corresponds to the toe-link, and the spring is represented by the line joining p55 and p56.

2.3 Frame Structure

A 1-D element is a line connecting two nodes, and such elements are formed together to create a frame structure[1]. Frame structures contain elements for which tensional, torsional, and bending effects all need to be considered. Therefore, an element with two ends is associated with six degrees of freedom (DOFs), resulting in a stiffness matrix involving 12 DOFs and producing an element stiffness matrix of order 12 [7].

[1] `https://2021.help.altair.com/2021/hwdesktop/hwx/topics/pre_processing/entities/elements_1d_r.htm`

The element stiffness matrix formulation differs for elements with uniform cross-sections and those with varying cross-sections.

2.3.1 Uniform Cross Section

The element with a uniform cross-section has a constant diameter throughout its length. This thesis focuses exclusively on elements with circular cross-sections, resulting in the constant parameters needed for the calculation of the stiffness matrix. The parameters involved in both the calculation of the stiffness matrix and the cross-section changes are as follows:

- Area
  - $A = \pi \cdot r^2$
- Polar moment of inertia
  - $J = \frac{\pi \cdot r^2}{2}$
- Second moments of inertia, Iy and Iz
  - $I_y = I_z = \frac{\pi \cdot r^4}{4}$

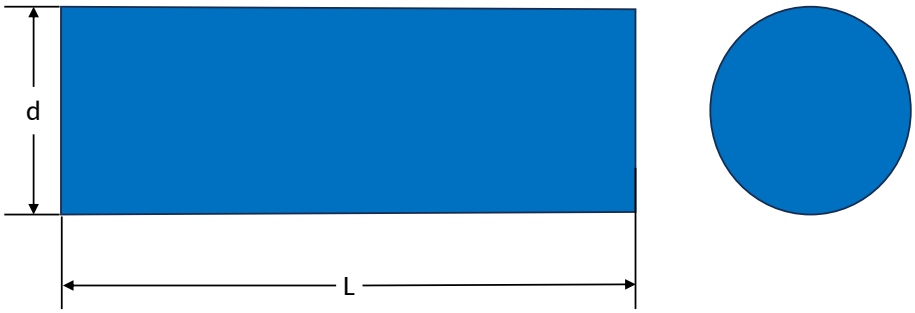

Figure 2.3: An element with a uniform circular cross-section.

where:

- r is the radius of the element,
- d is the diameter of the element, and
- L is the length of the element.

The stiffness matrix of an element (Figure 2.3) with a uniform cross-section is given

as [7],

$$K^e_{local} = \begin{bmatrix} \frac{EA}{L} & \cdot & \cdot & \cdot & \cdot & \cdot & -\frac{EA}{L} & \cdot & \cdot & \cdot & \cdot & \cdot \\ & \frac{12EI_z}{L^3} & \cdot & \cdot & \cdot & \frac{6EI_z}{L^2} & \cdot & -\frac{12EI_z}{L^3} & \cdot & \cdot & \cdot & \frac{6EI_z}{L^2} \\ & & \frac{12EI_y}{L^3} & \cdot & -\frac{6EI_y}{L^2} & \cdot & \cdot & \cdot & -\frac{12EI_y}{L^3} & \cdot & -\frac{6EI_y}{L^2} & \cdot \\ & & & \frac{GJ}{L} & \cdot & \cdot & \cdot & \cdot & \cdot & -\frac{GJ}{L} & \cdot & \cdot \\ & & & & \frac{4EI_y}{L} & \cdot & \cdot & \cdot & \frac{6EI_y}{L^2} & \cdot & \frac{2EI_y}{L} & \cdot \\ & & & & & \frac{4EI_z}{L} & \cdot & -\frac{6EI_z}{L^2} & \cdot & \cdot & \cdot & \frac{2EI_z}{L} \\ & & & & & & \frac{EA}{L} & \cdot & \cdot & \cdot & \cdot & \cdot \\ & & & \text{sym} & & & & \frac{12EI_z}{L^3} & \cdot & \cdot & \cdot & -\frac{6EI_z}{L^2} \\ & & & & & & & & \frac{12EI_y}{L^3} & \cdot & \frac{6EI_y}{L^2} & \cdot \\ & & & & & & & & & \frac{GJ}{L} & \cdot & \cdot \\ & & & & & & & & & & \frac{4EI_y}{L} & \cdot \\ & & & & & & & & & & & \frac{4EI_z}{L} \end{bmatrix}, \tag{2.1}$$

where the zeros are replaced by dots for readability and

- E: Young's modulus
- G: Shear modulus
- EA: Axial stiffness
- EI_y & EI_z: Bending stiffness about the y-axis and z-axis respectively.
- GJ: Torsional stiffness

2.3.2 Varying Cross Section

In this thesis, the element with a varying cross-section is considered to be linearly varying as illustrated in Figure 2.4. This type of cross-section changes diameter gradually from one end of the element to the other. The change in diameter at any distance x along the length L of the element is defined by the following equations:

$$d = d_1 + \Delta d \cdot \frac{x}{L} \tag{2.2}$$

$$\Delta d = d_2 - d_1 \tag{2.3}$$

Hence, the calculation of the stiffness matrix for this case needs to be done such that the parameters stated in the previous section account for the varying cross-section.

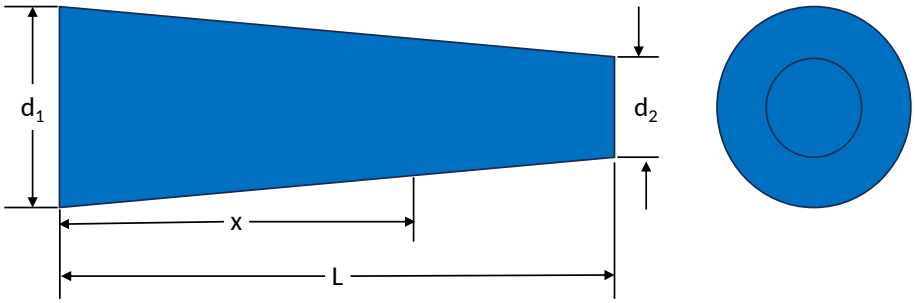

Figure 2.4: A linearly varying element with a circular cross-section.

2.3.2.1 Calculation of Flexibility Terms

In structural analysis, the flexibility terms are essential for defining the stiffness of non-prismatic elements. The flexibility method involves the calculation of these terms to derive the stiffness matrices for beam elements with varying cross-sections.

The flexibility matrix for a 3D non-prismatic beam element is given as [2]:

$$\mathbf{f} = \begin{bmatrix} f_{11} & 0 & 0 & 0 & 0 & 0 \\ 0 & f_{22} & 0 & 0 & 0 & f_{26} \\ 0 & 0 & f_{33} & 0 & -f_{35} & 0 \\ 0 & 0 & 0 & f_{44} & 0 & 0 \\ 0 & 0 & -f_{53} & 0 & f_{55} & 0 \\ 0 & f_{62} & 0 & 0 & 0 & f_{66} \end{bmatrix} \tag{2.4}$$

The flexibility terms in the flexibility matrix for a linearly varying circular cross-section are as follows:

The axial flexibility term is

$$f_{11} = \frac{4L}{\pi E d_1^2} \cdot \left(\frac{d_1}{d_2 - d_1} \right) \cdot \left(1 - \frac{d_1}{d_2} \right). \tag{2.5}$$

The torsional flexibility term is

$$f_{44} = \frac{32L}{3\pi G d_1^4} \cdot \left(\frac{d_1}{d_2 - d_1} \right) \cdot \left[1 - \left(\frac{d_1}{d_2} \right)^3 \right]. \tag{2.6}$$

The flexibility terms, f_{22}, f_{26}, f_{66} and f_{33}, f_{35}, f_{55} correspond to the bending defor-

mations with respect to the major axis **x** and minor axis **y** respectively, where

$$f_{22} = f_{33} = \frac{64L^3}{3\pi E d_1^4} \cdot \left(\frac{d_1}{d_2}\right)^3 + \frac{40L}{9\pi G d_1^2} \cdot \left(\frac{d_1}{d_2 - d_1}\right) \cdot \left(1 - \frac{d_1}{d_2}\right), \tag{2.7}$$

$$f_{26} = f_{35} = \frac{64L^2}{3\pi E d_1^4} \cdot \left\{ \left(\frac{d_1}{d_2}\right)^3 + 0.5 \cdot \left(\frac{d_1}{d_2 - d_1}\right)^2 \cdot \left[1 + \left(\frac{d_1}{d_2}\right)^2 - 2 \cdot \frac{d_1}{d_2}\right] \right\}, \tag{2.8}$$

$$f_{66} = f_{55} = \frac{64L}{3\pi E d_1^4} \cdot \left(\frac{d_1}{d_2 - d_1}\right) \cdot \left[1 - \left(\frac{d_1}{d_2}\right)^3\right]. \tag{2.9}$$

2.3.2.2 Axial and Torsional Stiffness Coefficients

The axial (r_{ax}) and torsional (r_j) stiffness coefficients are given as:

$$r_{ax} = \frac{1}{f_{11}}; \qquad r_j = \frac{1}{f_{44}}. \tag{2.10}$$

2.3.2.3 Major Bending-Stiffness Coefficients

The determinant (Det_x) of the flexibility terms for bending with respect to major axis x is given by

$$Det_x = f_{22} f_{66} - f_{26}^2. \tag{2.11}$$

The bending stiffness coefficients with respect to the major axis x are given by

$$r_{11x} = \frac{f_{22}}{Det_x}; \qquad r_{12x} = \frac{f_{26}L - f_{22}}{Det_x}, \tag{2.12}$$

$$r_{22x} = \frac{f_{66}L^2 - 2f_{26}L + f_{22}}{Det_x}; \qquad r_{aax} = \frac{r_{11x} + r_{22x} + 2r_{12x}}{L^2}, \tag{2.13}$$

$$r_{abx} = \frac{r_{11x} + r_{12x}}{L}; \qquad r_{bax} = \frac{r_{22x} + r_{12x}}{L}. \tag{2.14}$$

2.3.2.4 Minor Bending-Stiffness Coefficients

The determinant of the flexibility terms for bending with respect to minor axis y is given by

$$Det_y = f_{33} f_{35} - f_{35}^2. \tag{2.15}$$

The bending stiffness coefficients with respect to the minor axis y are given by

$$r_{11y} = \frac{f_{33}}{Det_y}; \qquad r_{12y} = \frac{f_{35}L - f_{33}}{Det_y}, \tag{2.16}$$

$$r_{22y} = \frac{f_{55}L^2 - 2f_{35}L + f_{33}}{Det_y}; \qquad r_{aay} = \frac{r_{11y} + r_{22y} + 2r_{12y}}{L^2}, \tag{2.17}$$

$$r_{aby} = \frac{r_{11y} + r_{12y}}{L}; \qquad r_{bay} = \frac{r_{22y} + r_{12y}}{L}. \tag{2.18}$$

2.3.2.5 Element Stiffness Matrix - Formulation

The stiffness matrix (K^e_{local}) in its local coordinates is defined with stiffness submatrices as

$$K^e_{local} = \begin{pmatrix} k_{11} & k_{12} \\ k_{21} & k_{22} \end{pmatrix}, \tag{2.19}$$

where the stiffness submatrices are given as

$$k_{11} = \begin{bmatrix} r_{ax} & 0 & 0 & 0 & 0 & 0 \\ 0 & r_{aax} & 0 & 0 & 0 & r_{abx} \\ 0 & 0 & r_{aay} & 0 & -r_{aby} & 0 \\ 0 & 0 & 0 & r_j & 0 & 0 \\ 0 & 0 & -r_{aby} & 0 & r_{11y} & 0 \\ 0 & r_{abx} & 0 & 0 & 0 & r_{11x} \end{bmatrix}, \tag{2.20}$$

$$k_{22} = \begin{bmatrix} r_{ax} & 0 & 0 & 0 & 0 & 0 \\ 0 & r_{aax} & 0 & 0 & 0 & -r_{bax} \\ 0 & 0 & r_{aay} & 0 & r_{bay} & 0 \\ 0 & 0 & 0 & r_j & 0 & 0 \\ 0 & 0 & r_{bay} & 0 & r_{22y} & 0 \\ 0 & -r_{bax} & 0 & 0 & 0 & r_{22x} \end{bmatrix}, \tag{2.21}$$

$$k_{12} = k_{21}^T = \begin{bmatrix} -r_{ax} & 0 & 0 & 0 & 0 & 0 \\ 0 & -r_{aax} & 0 & 0 & 0 & r_{bax} \\ 0 & 0 & -r_{aay} & 0 & -r_{bay} & 0 \\ 0 & 0 & 0 & -r_j & 0 & 0 \\ 0 & 0 & r_{aby} & 0 & r_{12y} & 0 \\ 0 & -r_{abx} & 0 & 0 & 0 & r_{12x} \end{bmatrix}. \tag{2.22}$$

Thus, the element stiffness matrix for the considered 3D-element (Figure 2.4) is

$$K^e_{local} = \begin{bmatrix} r_{ax} & \cdot & \cdot & \cdot & \cdot & \cdot & -r_{ax} & \cdot & \cdot & \cdot & \cdot & \cdot \\ & r_{aax} & \cdot & \cdot & \cdot & r_{abx} & \cdot & -r_{aax} & \cdot & \cdot & \cdot & r_{bax} \\ & & r_{aay} & \cdot & -r_{aby} & \cdot & \cdot & \cdot & -r_{aay} & \cdot & -r_{bay} & \cdot \\ & & & r_j & \cdot & \cdot & \cdot & \cdot & \cdot & -r_j & \cdot & \cdot \\ & & & & r_{11y} & \cdot & \cdot & \cdot & r_{aby} & \cdot & r_{12y} & \cdot \\ & & & & & r_{11x} & \cdot & -r_{abx} & \cdot & \cdot & \cdot & r_{12x} \\ & & & & & & r_{ax} & \cdot & \cdot & \cdot & \cdot & \cdot \\ & & \text{sym} & & & & & r_{aax} & \cdot & \cdot & \cdot & -r_{bax} \\ & & & & & & & & r_{aay} & \cdot & r_{bay} & \cdot \\ & & & & & & & & & r_j & \cdot & \cdot \\ & & & & & & & & & & r_{22y} & \cdot \\ & & & & & & & & & & & r_{22x} \end{bmatrix}. \tag{2.23}$$

2.4 Transformation Matrix

The transformation matrix is a fundamental tool in finite element analysis for converting the stiffness matrix of an element from its local coordinate system to the global coordinate system. Initially, the stiffness matrices for individual elements are computed in their respective local coordinate systems. Then, the element is moved from its local coordinate system to its corresponding position in the global coordinate system using the transformation matrix [5]. This transformation matrix (T) is given by

$$T = \begin{bmatrix} r & 0 & 0 & 0 \\ 0 & r & 0 & 0 \\ 0 & 0 & r & 0 \\ 0 & 0 & 0 & r \end{bmatrix}, \tag{2.24}$$

where r is a matrix consisting of the direction cosines that describe the orientation of the local coordinate system with respect to the global coordinate system and given by

$$r = \begin{bmatrix} C_{Xx} & C_{Yx} & C_{Zx} \\ C_{Xy} & C_{Yy} & C_{Zy} \\ C_{Xz} & C_{Yz} & C_{Zz} \end{bmatrix}. \tag{2.25}$$

Here we consider the y-axis to be always normal to the x-Z plane, hence it is sufficient to specify the position of the local coordinate system (x-y-z) with respect to the global (X-Y-Z) by using the direction cosines of the x-axis only.

The calculation of the direction cosines of the x-axis with respect to the global axes is given as

$$C_{Xx} = \frac{\vec{a} \cdot \vec{i}}{|\vec{a}| \cdot \left|\vec{i}\right|}, \tag{2.26}$$

$$C_{Yx} = \frac{\vec{a} \cdot \vec{j}}{|\vec{a}| \cdot \left|\vec{j}\right|}, \tag{2.27}$$

$$C_{Zx} = \frac{\vec{a} \cdot \vec{k}}{|\vec{a}| \cdot \left|\vec{k}\right|}, \tag{2.28}$$

where $\vec{a}$ is the vector formed by joining the two nodes of the element, given by

$$\vec{a} = (x_2 - x_1)\vec{i} + (y_2 - y_1)\vec{j} + (z_2 - z_1)\vec{k}, \tag{2.29}$$

where

- $\vec{i}$, $\vec{j}$, and $\vec{k}$ are the unit vectors in x, y, and z-axes respectively.

To fully define the transformation matrix, we also need the direction cosines for the y and z-axes. They can be derived using the relationships:

$$C_{Xy} = -\frac{C_{Yx}}{D}; \qquad C_{Yy} = \frac{C_{Xx}}{D}; \qquad C_{Zy} = 0, \tag{2.30}$$

$$C_{Xz} = -\frac{C_{Xx} \cdot C_{Zx}}{D}; \qquad C_{Yz} = -\frac{C_{Yx} \cdot C_{Zx}}{D}; \qquad C_{Zz} = D, \tag{2.31}$$

where

$$D = \sqrt{C_{Xx}^2 + C_{Yx}^2}. \tag{2.32}$$

Using (2.24), the local stiffness matrix (K_{local}^e) can be transformed into the global stiffness matrix (K_{global}^e) and given by

$$K_{global}^e = T^{-1} \cdot K_{local}^e \cdot T. \tag{2.33}$$

This equation ensures that the local stiffness contributions of each element are accurately mapped to the global coordinate system, allowing for the assembly of the global stiffness matrix necessary for structural analysis.

2.5 Describing a Local Coordinate System

The frame structure needs to be constrained at the nodes. For the rear knuckle considered in this thesis, the local coordinate systems are defined at the nodes $Pt5$, $Pt6$, and $Pt12$ (Figure 2.2), with the local x-axis oriented in the direction of the corresponding link arms. Defining a local coordinate system at these nodes allows for a more accurate and detailed analysis of the forces and movements within the frame structure.

To constrain the movement in the local coordinate system, we use a rotation matrix based on Euler angles. This matrix facilitates the transformation of coordinates from the global system to the local system, enabling precise control over the degrees of freedom at each node. By applying this rotational transformation, we ensure that the constraints are accurately imposed in the local coordinate directions, which is essential for correctly simulating the behavior of the knuckle under various load conditions.

2.5.1 Rotation Matrix

Let the Euler angles ϕ, θ, and ψ represent the rotation angles about the x, y, and z axes, respectively. These angles are used to define the orientation of the local coordinate system with respect to the global coordinate system. The rotation matrices corresponding to these angles describe how a vector in the global coordinate system can be transformed into the local coordinate system.

a) Rotation about the x-axis by an angle ϕ:

$$R_x(\phi) = \begin{bmatrix} 1 & 0 & 0 \\ 0 & \cos(\phi) & -\sin(\phi) \\ 0 & \sin(\phi) & \cos(\phi) \end{bmatrix} \tag{2.34}$$

This matrix represents a rotation that leaves the x-component of a vector unchanged while rotating the y and z components in the yz-plane.

b) Rotation about the y-axis by an angle θ:

$$R_y(\theta) = \begin{bmatrix} \cos(\theta) & 0 & \sin(\theta) \\ 0 & 1 & 0 \\ -\sin(\theta) & 0 & \cos(\theta) \end{bmatrix} \tag{2.35}$$

This matrix represents a rotation that leaves the y-component of a vector unchanged while rotating the x and z components in the xz-plane.

c) Rotation about the z-axis by an angle ψ:

$$R_z(\psi) = \begin{bmatrix} \cos(\psi) & -\sin(\psi) & 0 \\ \sin(\psi) & \cos(\psi) & 0 \\ 0 & 0 & 1 \end{bmatrix} \tag{2.36}$$

This matrix represents a rotation that leaves the z-component of a vector unchanged while rotating the x and y components in the xy-plane.

2.6 Direct Stiffness Method

The Direct Stiffness Method is used in this thesis, where the stiffness matrix (K) constitutes the stiffness properties of all the elements in the structure. The structure's unknown displacement is then found using the following formula:

$$F = K \cdot u, \tag{2.37}$$

$$\Rightarrow u = K^{-1} \cdot F, \tag{2.38}$$

where

- K is the global stiffness matrix of the whole frame structure,
- F is a vector of known nodal forces, and
- u is the vector of unknown nodal displacements.

2.7 Kinematic Stiffness Targets

The knuckle is tested to check whether it meets the stiffness targets for different kinematic parameters. Figure 2.5[2] illustrates the forces and moments acting on a wheel.

[2] `https://www.researchgate.net/figure/Tire-forces-and-moments_fig3_226822444`

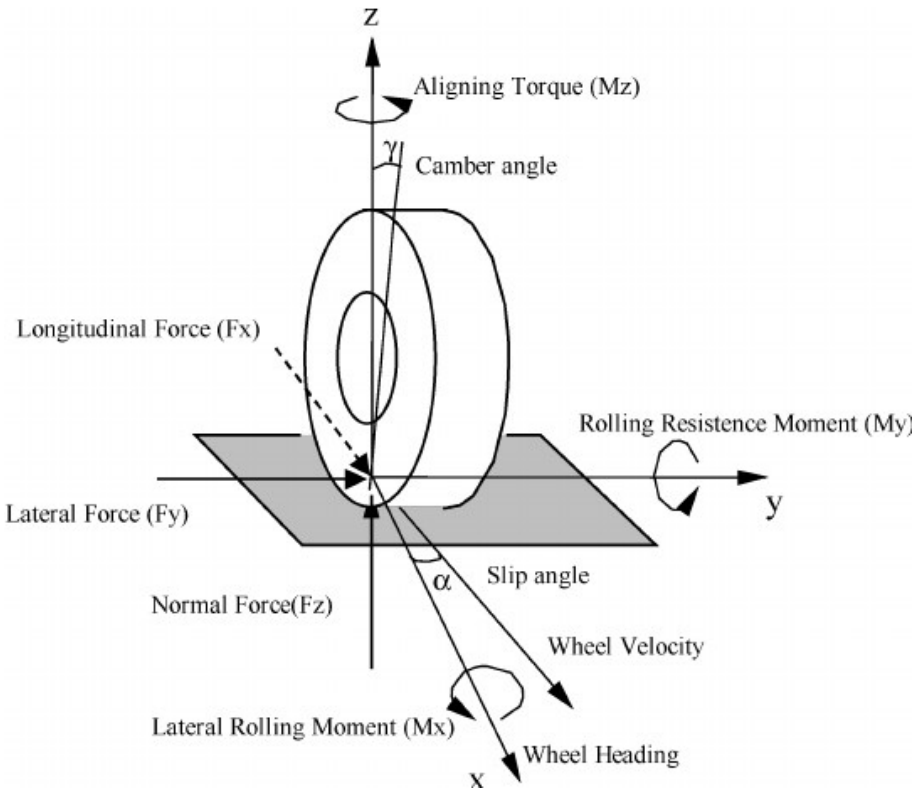

Figure 2.5: Forces and moments acting on a wheel.

The thesis focuses on the following kinematic cases and approximates the corresponding stiffness values.

2.7.1 Camber Stiffness

Camber stiffness is a fundamental characteristic evaluated in this study to assess the knuckle's ability to resist changes in camber angle. The camber angle plays a pivotal role in maintaining consistent tire contact with the road surface, thereby influencing the vehicle's grip, stability, and handling dynamics.

2.7.2 Aligning Torque Stiffness

Aligning torque stiffness pertains to the knuckle's resistance against forces that attempt to alter the wheel's steering angle, particularly during maneuvers such as cornering where, lateral forces are pronounced. This stiffness parameter is crucial for ensuring precise steering response and stability, as it directly influences the vehicle's ability to maintain directional control and cornering performance.

3

Methods

3.1 Reaction Force Calculation

The four-link suspension system shown in Figure 2.2 is considered with the earlier assumptions. Here, we discuss the methodology to find the reaction forces at the outer hardpoints for an applied force at the wheel contact point. The reaction forces are essential to understand as they directly influence the overall structural integrity of the knuckle. These forces are calculated by analyzing the equilibrium of the system, taking into account the applied loads and the geometry of the suspension links. The procedure involves applying the known force at the wheel contact point and using static equilibrium equations to solve for the unknown reaction forces at the hardpoints. This analysis helps in determining the distribution of forces on the hardpoints.

3.1.1 Contact Point Calculation

The wheel contact point is a critical aspect in the study of vehicle dynamics and suspension design. This point, where the tire meets the road surface, serves as the primary interface for transmitting forces between the vehicle and the ground. These forces include vertical loads due to the vehicle's weight, lateral forces from cornering, and longitudinal forces from acceleration and braking. The behavior at the wheel contact point significantly influences the overall handling, stability, and ride comfort of the vehicle.

However, in this thesis, the analysis is confined to the static behavior of the suspension system. The wheel contact point (CP) at a static position can be calculated with static camber and toe angle as,

$$CP = Pt9 + R_W \cdot \begin{pmatrix} -\sin(\gamma) \cdot \sin(\delta) \\ \sin(\gamma) \cdot \cos(\delta) \\ -\cos(\gamma) \end{pmatrix}, \tag{3.1}$$

where

- R_W is the wheel radius of the vehicle,
- γ is the static camber angle,
- δ is the static toe angle, and
- $Pt9$ is the wheel center (Figure 2.2).

3.1.2 Force and Moment Equilibrium

The moment at Pt6 due to the contact point forces is calculated as,

$$\vec{M_{cp}} = (CP - Pt6) \times \vec{F}. \tag{3.2}$$

The direction vectors for the coefficient matrix (A) are defined as follows

$$\hat{d_5} = \frac{(Pt5 - Pt3)}{d_{5-3}}; \tag{3.3}$$

$$\vec{b_{56}} = Pt5 - Pt6; \qquad \vec{dt_{56}} = \vec{b_{56}} \times \hat{d_5}, \tag{3.4}$$

where

- d_{5-3} is the distance between the points $Pt5$ and $Pt3$.

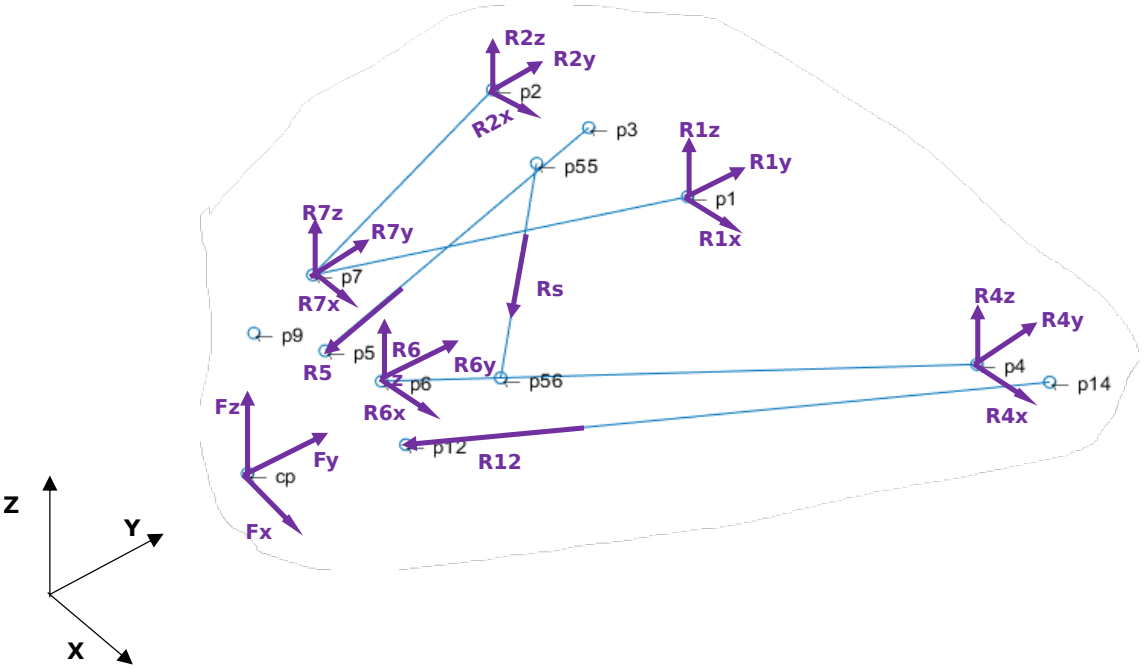

Figure 3.1: Free body diagram of the four-link suspension system.

The equations to solve for the reaction forces at the outer hardpoints are found using the force and moment balance equations for the suspension system illustrated by Figure 3.1 and are represented in the form of a linear matrix of the form

$$A \cdot X = B, \tag{3.5}$$

where

- X is a vector of nodal reaction forces,
- B is the applied wheel contact forces, and

- A is the coefficient matrix.

$$X = \begin{pmatrix} R7x \\ R7y \\ R7z \\ R6x \\ R6y \\ R6z \\ R5 \\ R12 \\ R4x \\ R4y \\ R4z \\ Rs \\ R1x \\ R1y \\ R1z \\ R2x \\ R2y \\ R2z \end{pmatrix}; \qquad B = \begin{pmatrix} Fx \\ Fy \\ Fz \\ -(M_{cp})_x + M_x \\ -(M_{cp})_y + M_y \\ -(M_{cp})_z + M_z \\ 0 \\ 0 \\ 0 \\ 0 \\ 0 \\ 0 \\ 0 \\ 0 \\ 0 \\ 0 \\ 0 \\ 0 \end{pmatrix}. \tag{3.6}$$

$$A = \begin{bmatrix} 1 & \cdot & \cdot & 1 & \cdot & \cdot & d_{5x} & d_{12x} & \cdot & \cdot & \cdot & \cdot & \cdot & \cdot & \cdot & \cdot & \cdot & \cdot \\ \cdot & 1 & \cdot & \cdot & 1 & \cdot & d_{5y} & d_{12y} & \cdot & \cdot & \cdot & \cdot & \cdot & \cdot & \cdot & \cdot & \cdot & \cdot \\ \cdot & \cdot & 1 & \cdot & \cdot & 1 & d_{5z} & d_{12z} & \cdot & \cdot & \cdot & \cdot & \cdot & \cdot & \cdot & \cdot & \cdot & \cdot \\ dt_{7ax} & dt_{7bx} & dt_{7cx} & \cdot & \cdot & \cdot & dt_{5x} & dt_{12x} & \cdot & \cdot & \cdot & \cdot & \cdot & \cdot & \cdot & \cdot & \cdot & \cdot \\ dt_{7ay} & dt_{7bx} & dt_{7cx} & \cdot & \cdot & \cdot & dt_{5y} & dt_{12x} & \cdot & \cdot & \cdot & \cdot & \cdot & \cdot & \cdot & \cdot & \cdot & \cdot \\ dt_{7az} & dt_{7bx} & dt_{7cx} & \cdot & \cdot & \cdot & dt_{5z} & dt_{12x} & \cdot & \cdot & \cdot & \cdot & \cdot & \cdot & \cdot & \cdot & \cdot & \cdot \\ \cdot & \cdot & \cdot & -1 & \cdot & \cdot & \cdot & \cdot & 1 & \cdot & \cdot & d_{56x} & \cdot & \cdot & \cdot & \cdot & \cdot & \cdot \\ \cdot & \cdot & \cdot & \cdot & -1 & \cdot & \cdot & \cdot & \cdot & 1 & \cdot & d_{56y} & \cdot & \cdot & \cdot & \cdot & \cdot & \cdot \\ \cdot & \cdot & \cdot & \cdot & \cdot & -1 & \cdot & \cdot & \cdot & \cdot & 1 & d_{56z} & \cdot & \cdot & \cdot & \cdot & \cdot & \cdot \\ \cdot & \cdot & \cdot & dt_{64ax} & dt_{64bx} & dt_{64cx} & \cdot & \cdot & \cdot & \cdot & \cdot & dt56_{564x} & \cdot & \cdot & \cdot & \cdot & \cdot & \cdot \\ \cdot & \cdot & \cdot & dt_{64ay} & dt_{64by} & dt_{64cy} & \cdot & \cdot & \cdot & \cdot & \cdot & dt56_{564y} & \cdot & \cdot & \cdot & \cdot & \cdot & \cdot \\ \cdot & \cdot & \cdot & dt_{64az} & dt_{64bz} & dt_{64cz} & \cdot & \cdot & \cdot & \cdot & \cdot & dt56_{564z} & \cdot & \cdot & \cdot & \cdot & \cdot & \cdot \\ -1 & \cdot & \cdot & 1 & \cdot & \cdot & \cdot & \cdot & \cdot & \cdot & \cdot & \cdot & 1 & \cdot & \cdot & 1 & \cdot & \cdot \\ \cdot & -1 & \cdot & 1 & \cdot & \cdot & \cdot & \cdot & \cdot & \cdot & \cdot & \cdot & \cdot & 1 & \cdot & \cdot & 1 & \cdot \\ \cdot & \cdot & -1 & 1 & \cdot & \cdot & \cdot & \cdot & \cdot & \cdot & \cdot & \cdot & \cdot & \cdot & 1 & \cdot & \cdot & 1 \\ dt_{71ax} & dt_{71bx} & dt_{71cx} & \cdot & \cdot & \cdot & \cdot & \cdot & \cdot & \cdot & \cdot & \cdot & \cdot & \cdot & \cdot & dt_{21ax} & dt_{21bx} & dt_{21cx} \\ dt_{71ay} & dt_{71by} & dt_{71cy} & \cdot & \cdot & \cdot & \cdot & \cdot & \cdot & \cdot & \cdot & \cdot & \cdot & \cdot & \cdot & dt_{21ay} & dt_{21by} & dt_{21cy} \\ dt_{71az} & dt_{71bz} & dt_{71cz} & \cdot & \cdot & \cdot & \cdot & \cdot & \cdot & \cdot & \cdot & \cdot & \cdot & \cdot & \cdot & dt_{21az} & dt_{21bz} & dt_{21cz} \end{bmatrix}. \tag{3.7}$$

The resultant force vector can be found from

$$X = A^{-1} \cdot B. \tag{3.8}$$

The nodal reaction forces $R7$, $R12$, $R6$, and $R5$ are found from the resultant force vector X and then used as prescribed forces to find the nodal displacements.

3.2 Knuckle Structure Formation

The five outer hardpoints are joined together using 3D beams of uniform and linearly varying circular cross-sections. The beams are joined to the outer hardpoints (nodes) in such a way that it can be useful in approximating the stiffness of the knuckle.

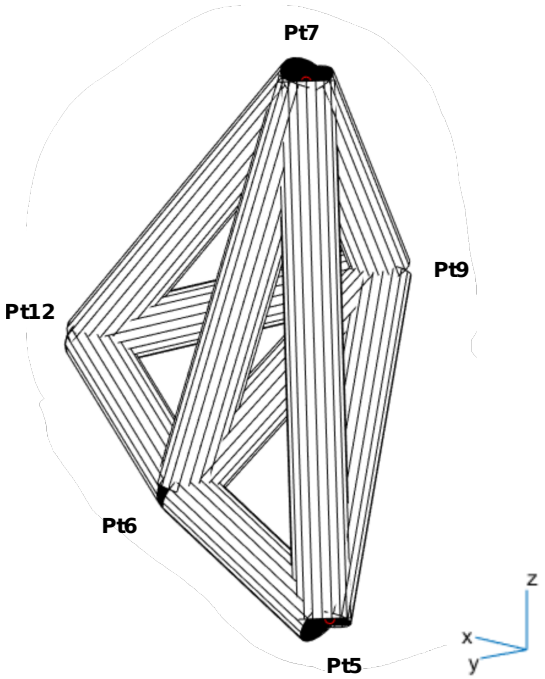

Figure 3.2: Frame structure with uniform cross-sections.

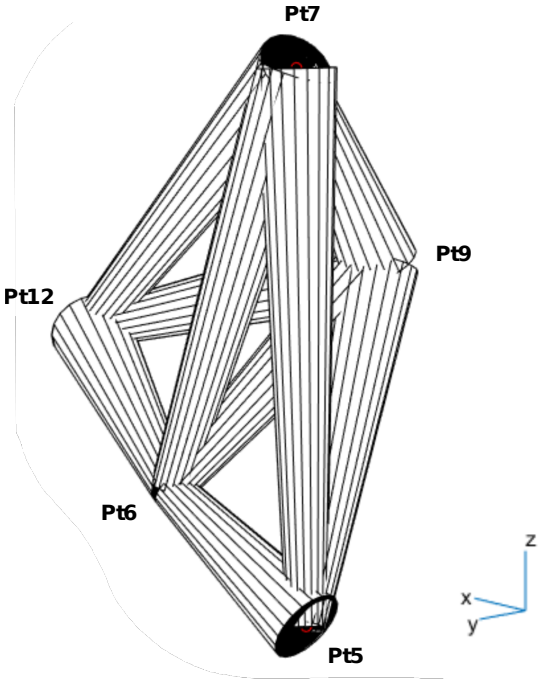

Figure 3.3: Frame structure with linearly varying cross-sections.

Figures 3.2 and 3.3 respectively illustrate the frame structures formed with 3D beam elements of uniform and linearly varying circular cross-sections.

With the definition of geometry and material properties of the beam, the global stiffness matrix of the whole frame structure is assembled and the steps involved are as follows:

a) Identifying the Degrees of Freedom (DOFs) :

Each node in the frame structure has 6 DOFs and in total there are 30 DOFs for the frame structure with the $Pt9$ having the DOFs numbered from 1 to 6 and $Pt7$ from 7 to 12 and then the same continues in the order $Pt12$, $Pt6$, and $Pt5$.

b) Element Stiffness Matrix (K^e_{local}):

The element stiffness matrix for each element is derived from the material properties and geometry of the element. This matrix is defined in the local coordinate system of the element and can be found using the equations (2.1) or (2.23), depending on the type of elements.

c) Transformation to Global Coordinate System (K^e_{global}):

The element stiffness matrix is transformed from its local coordinate system to the global coordinate system using the transformation matrix (T) as given by the equation (2.33).

d) Assembly into the Global Stiffness Matrix (K):

The global stiffness matrix K is assembled by summing the contributions of each element stiffness matrix K^e_{global} according to the global DOFs. The process involves:

- Identifying the global DOF indices corresponding to the local DOFs of each element.
- Placing the entries of K^e_{global} into the global stiffness matrix K at the appropriate positions.

The MATLAB function to calculate the global stiffness matrices of the individual elements K^e_{global} and the whole structure's stiffness matrix K is provided in Appendix A.

3.3 Calculation of nodal displacements

The global stiffness matrix K relates the nodal displacements u to the applied forces F through the equation $K \cdot u = F$. When constraints (boundary conditions) are applied, the system must be modified to account for the fixed DOFs.

The process involves separating the DOFs into constrained and unconstrained sets and then solving for the displacements of the unconstrained DOFs. The steps are as follows:

a) Identifying Constrained and Unconstrained DOFs:

Constrained DOFs are those where boundary conditions are applied (e.g., fixed supports). Unconstrained DOFs are free to move under the applied loads.

b) Partitioning the System:

Partition the global stiffness matrix K and force vector F into submatrices and subvectors corresponding to constrained and unconstrained DOFs so that

$$\begin{bmatrix} K_{cc} & K_{cu} \\ K_{uc} & K_{uu} \end{bmatrix} \begin{bmatrix} u_c \\ u_u \end{bmatrix} = \begin{bmatrix} F_c \\ F_u \end{bmatrix}, \tag{3.9}$$

where

- u_c and F_c are the displacement and force vectors for constrained DOFs.
- u_u and F_u are the displacement and force vectors for unconstrained DOFs.

c) Solving for Unconstrained Displacements:

Since the displacements u_c of constrained DOFs are known (zero for fixed supports),

the equation reduces to:

$$K_{uu} \cdot u_u = F_u \tag{3.10}$$

The displacements u_u of the unconstrained DOFs are then calculated by:

$$u_u = K_{uu}^{-1} \cdot F_u \tag{3.11}$$

Here, K_{uu}^{-1} is the inverse of the submatrix of the global stiffness matrix corresponding to the unconstrained DOFs.

3.4 Modelling Suspension System in ADAMS Car

For validating the results from the mathematical model to find the nodal reaction forces, the four-link suspension system was modeled on the ADAMS car software. The following simplifications were done in the model to compare the results from the mathematical model:

- The stiffness of the spring and bushings are considered high enough to consider it as a rigid component and there is no damper in the system.
- The forces are applied at the wheel contact point and the wheel mass is considered as low as possible.
- The link arms are rigid and massless.
- The static analysis is done to evaluate the reaction forces at the outer hardpoints.

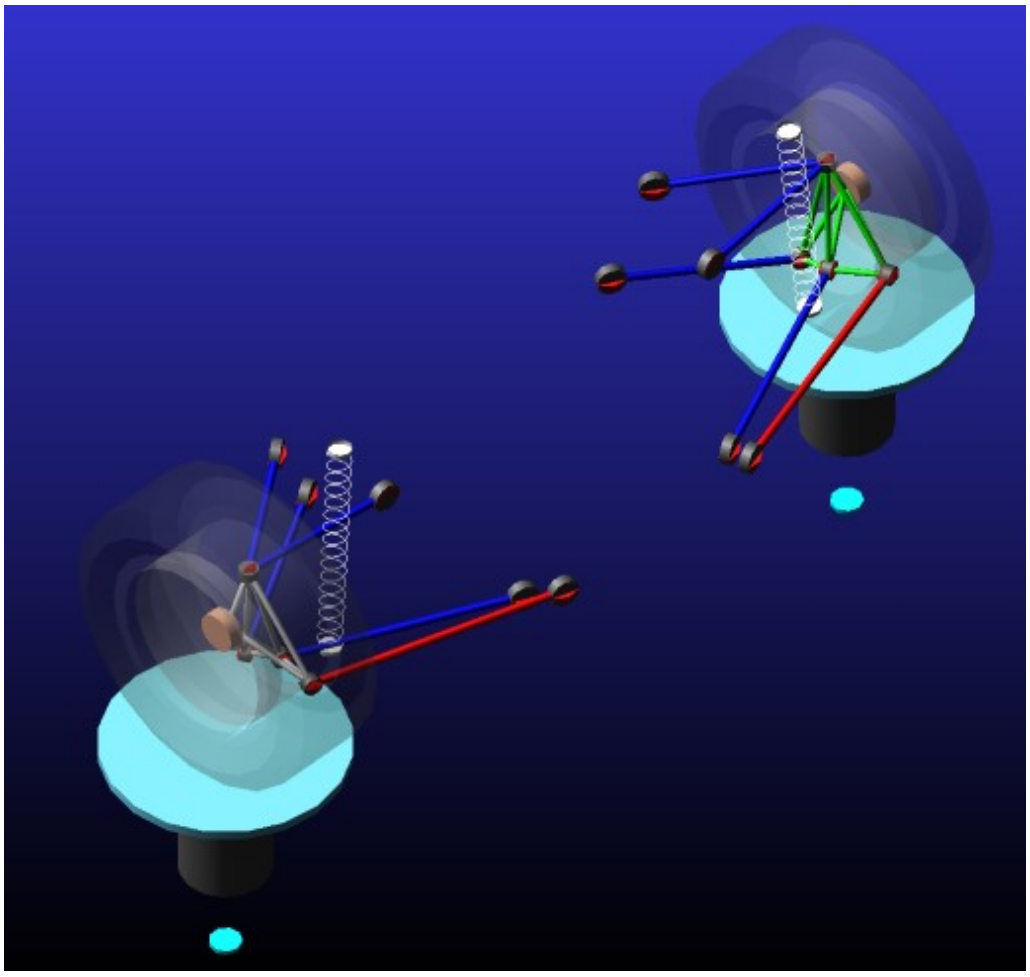

Figure 3.4: ADAMS Car model of the four-link suspension system.

3.5 Finite Element Analysis of Frame Structure in NX

To validate the results from the mathematical model for finding the nodal displacements of the frame structure, the frame structure formed by joining the outer hardpoints is modeled in the Siemens NX FE Software. The frame structure modeled in Siemens NX software is shown in Figure 3.5. The following methodology is followed to model the structure:

- The coordinates are first defined and joined using line geometries.
- The geometry is then meshed with 1D elements of type CBEAM, with tapered circular cross-sections, and this CBEAM element is chosen for its capability to model a tapered cross-section[1].
- The constrained DOFs are defined after defining the local coordinate system. It is followed by the application of prescribed forces.

[1] `https://simulatemore.mscsoftware.com/choosing-the-right-finite-element-msc-nastran/`

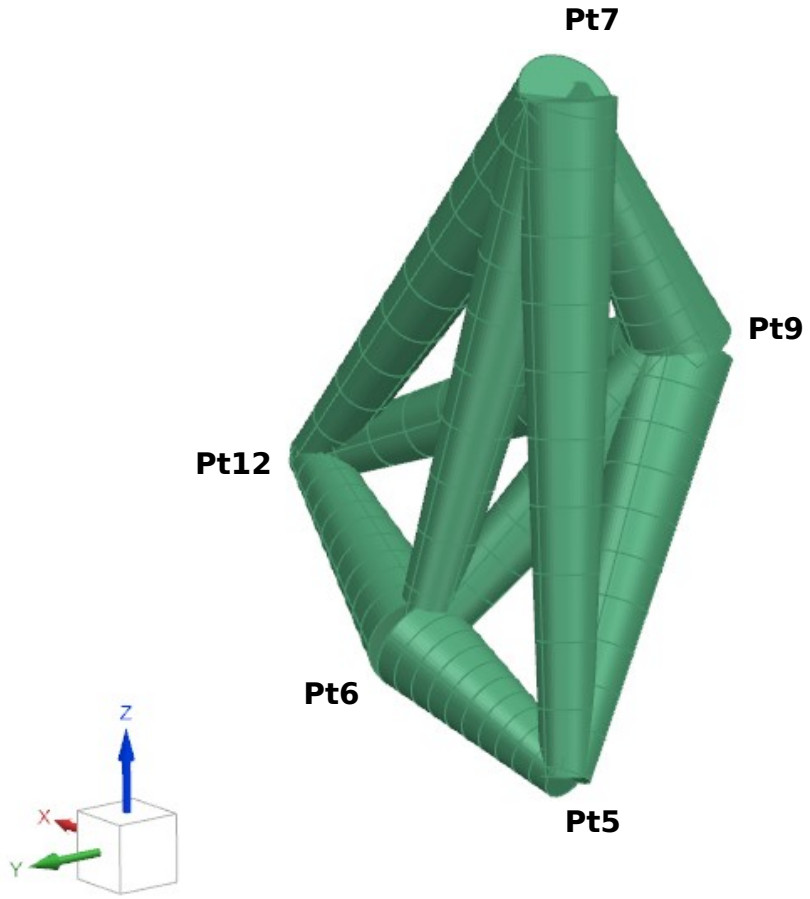

Figure 3.5: Frame Structure in Siemens NX Finite Element Software.

4

Results

In this chapter, we have discussed the validation of our mathematical model and then the comparison of the mathematical model with the finite element mode of the knuckle.

4.1 Validation

The mathematical model for both the reaction forces and the frame structure has been validated before comparing the mathematical model with the FE model of the knuckle.

4.1.1 Nodal Reaction Forces

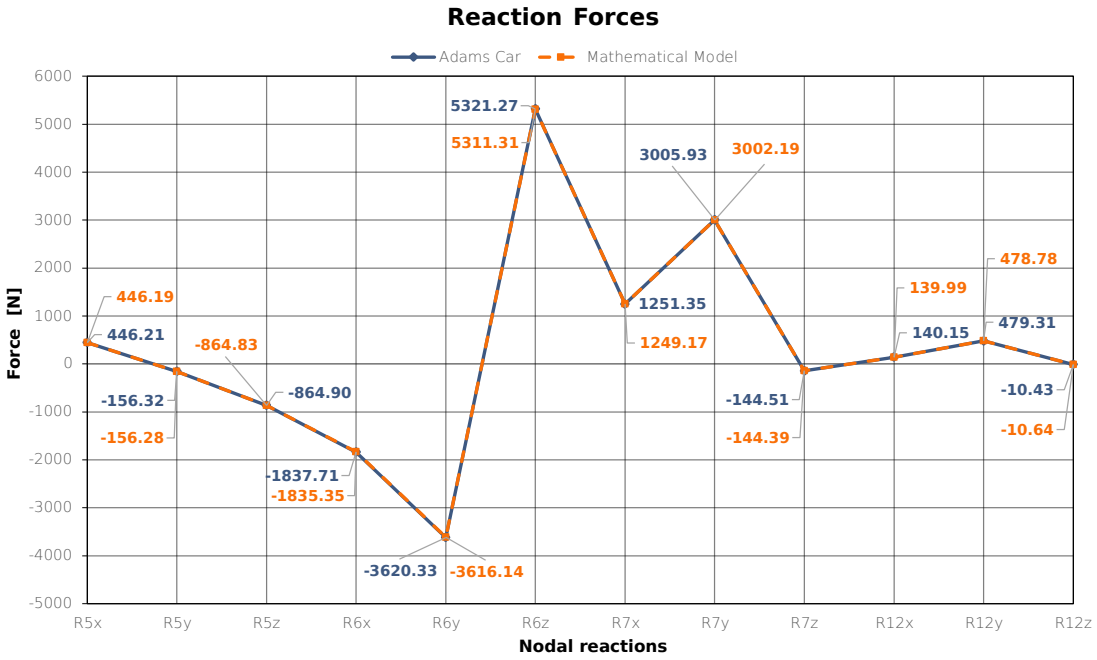

Figure 4.1: Reaction forces at the nodes from the mathematical model and Adams Car software.

Figure 4.1 illustrates the nodal reaction forces from both the mathematical model and the ADAMS Car model. For this analysis, a lateral force of 1000 [N] and a vertical load of 5000 [N] were applied at the wheel contact point. Based on the above Figure 4.1, we can conclude that the mathematical model correlates well with the ADAMS Car model and is thus validated.

4.1.2 Nodal Displacement

The mathematical model to find the nodal displacements is first validated with a single element and then with the frame structure.

4.1.2.1 Single Element

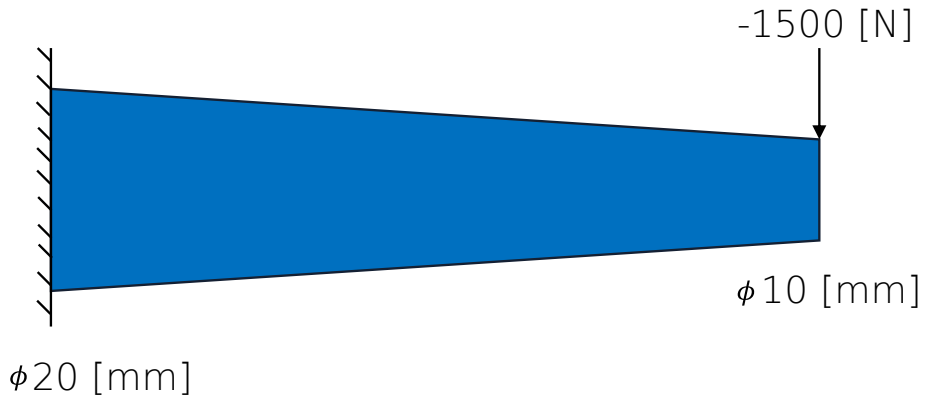

Figure 4.2: Continous cantilever beam element.

Figure 4.3: Stepped cantilever beam element.

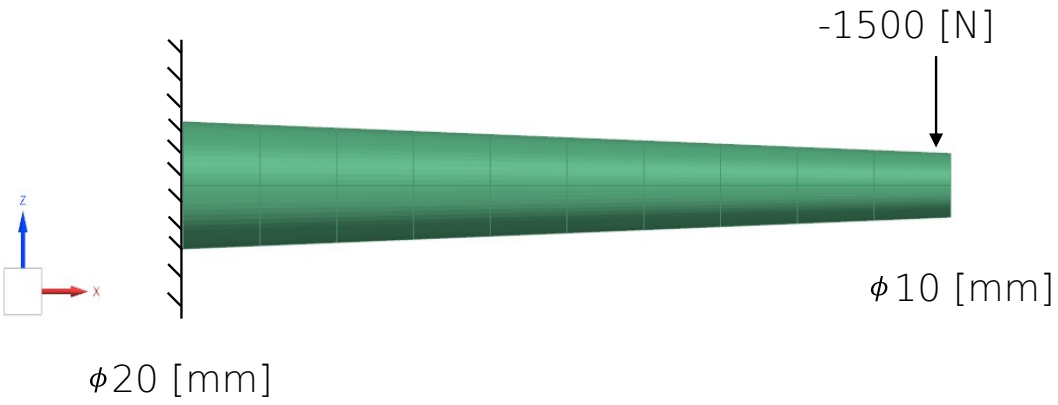

Figure 4.4: Finite Element model of the cantilever beam element.

The elements with varying cross-sections can be mathematically modeled as a single a) continuous beam and b) stepped beam. In the case of a continuous beam element, the element stiffness matrix (K^e_{local}) can be computed based on the equation (2.23). For the stepped beam elements, each discretized part is made up of beam elements with a uniform cross-section, and the element stiffness matrix (K^e_{local}) is computed using equation (2.1).

In this analysis, a cantilever beam of length 0.3 [m] has a linearly varying circular cross-section with ϕ 20 [mm] on its fixed end and ϕ 10 [mm] on its free end. A point load of -1500 [N] in the z-direction is applied to the beam. This same setup is modeled using a continuous beam element, stepped beam element, and Siemens NX FE Software.

The continuous beam element, stepped beam element, and the model built in FE software is shown in Figure 4.4.

The stepped beam model and the FE model can be discretized into several parts to refine the results and the comparison of vertical displacements using different models is shown in Figure 4.5.

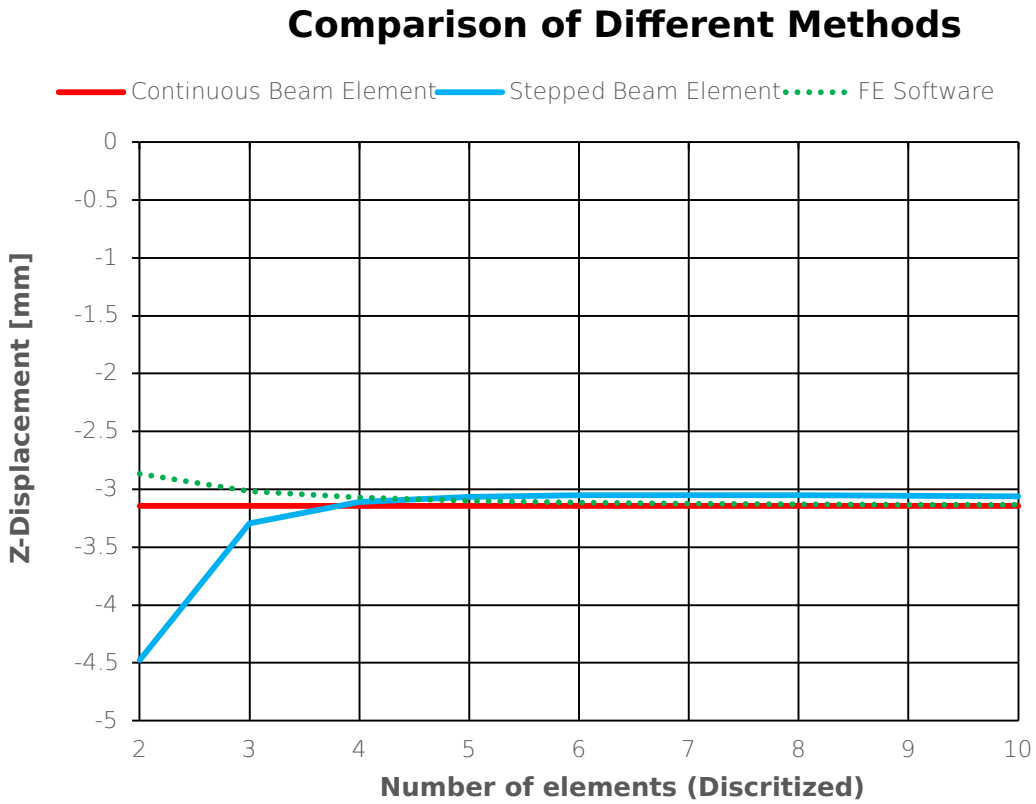

Figure 4.5: Comparison of vertical displacements from different models.

From Figure 4.5, we can infer that over 6 discretized elements in the stepped beam model and FE model, the results from all the models converge. Therefore, we can conclude that the mathematical model correlates with the FE model. It is also worth mentioning that the stepped beam element takes 30% more time to compute than the continuous beam model. Since more elements and an increased number of

discretizations will increase the complexity of tuning the parameters like diameters, we proceed further with the continuous beam model.

4.1.2.2 Frame Structure

The mathematical model for the frame structure is validated with the FE model in this section, and both models are illustrated in Figures 4.6 and 4.7.

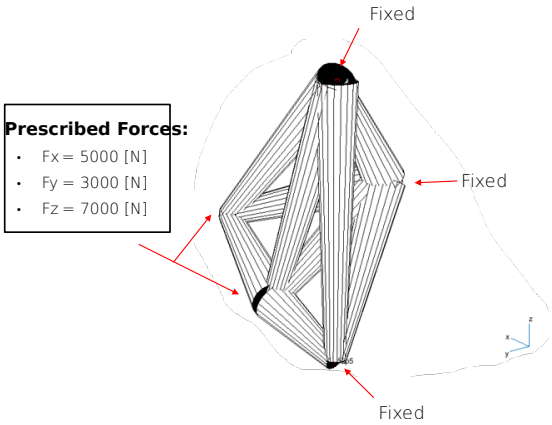

Figure 4.6: Mathematical model of the frame structure.

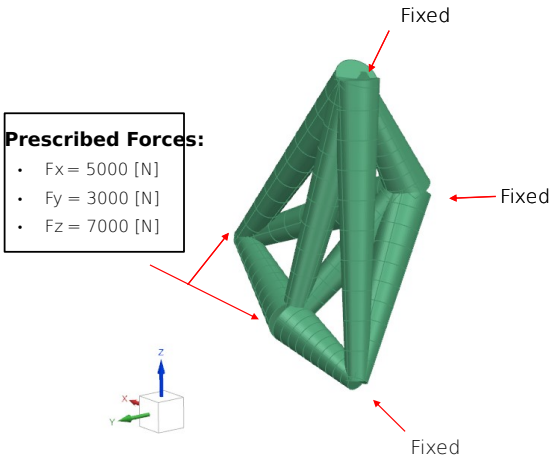

Figure 4.7: Finite Element model of the frame structure.

F_x	5000 [N]
F_y	3000 [N]
F_z	7000 [N]

Table 4.1: Prescribed forces on the free nodes.

The nodes Pt9, Pt7, and Pt5 are fixed and the prescribed forces shown in Table 4.1 are applied on the free nodes Pt6 and Pt12.

From Figure 4.8 we can infer that in both Pt6 and Pt12, the deformation from the FE model correlates well with the continuous beam mathematical model. The results from the FE model converge with discretized parts n=10 and we can see a deviation in results with a reduced number of discretized parts (n=1 and n=5).

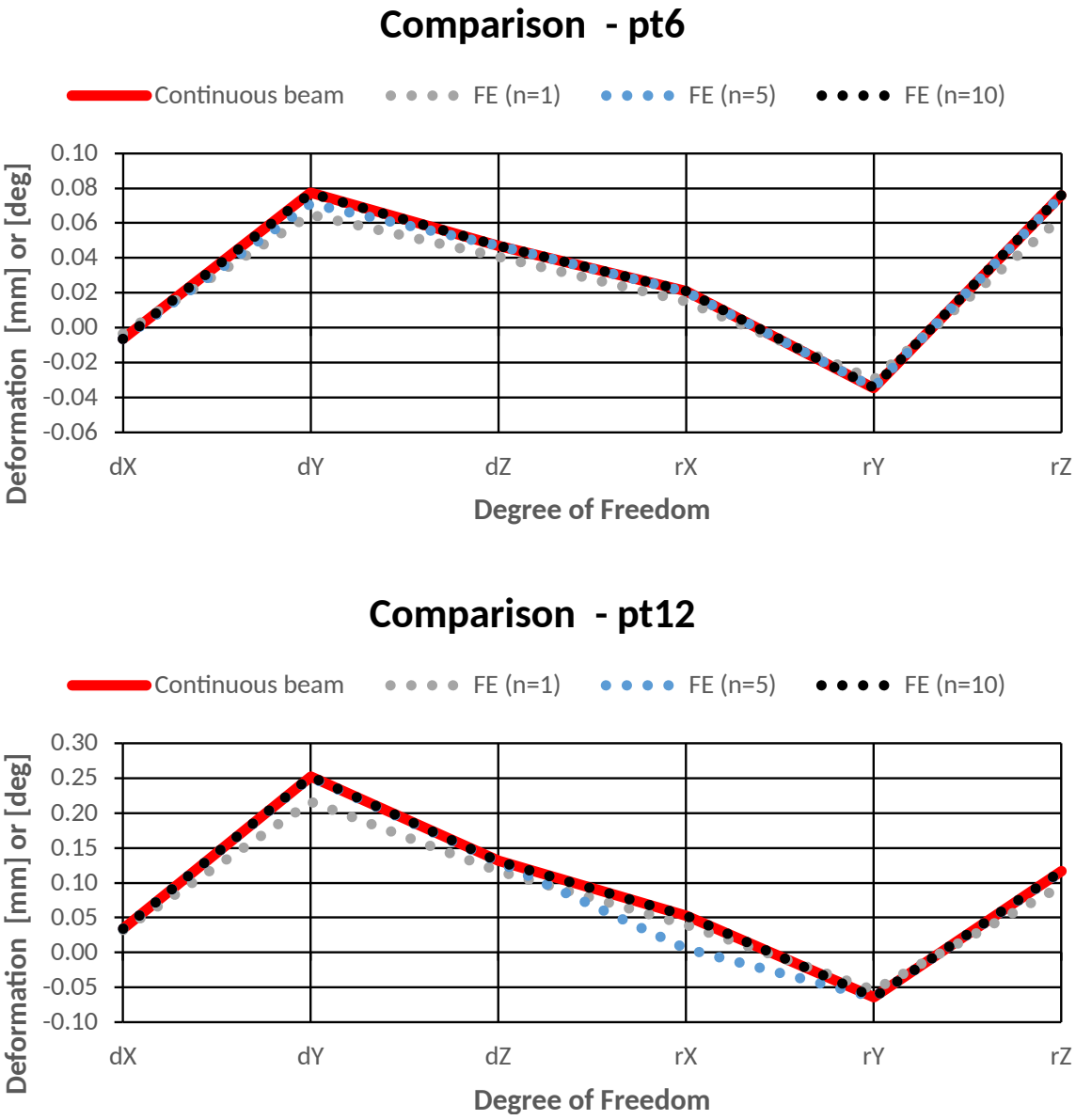

Figure 4.8: Comparison of deformation at the free nodes Pt6 and Pt12.

The continuous beam model has been validated for both the single-element cantilever beam and the frame structure.

4.2 Comparison

In this section, the mathematical model will be correlated with the results from the FE knuckle model. The stiffness results of the Finite Element knuckle were provided by Volvo Car Corporation and were used in this section.

The geometry of the individual elements has been manually tuned to get stiffness results within the accepted range of deviation and have a reasonable mass. Figure 4.9 illustrates the naming scheme of every single 3D beam element in the frame

structure. In Tables 4.2 and 4.3, each column corresponds to the diameters d_1 and d_2 of the beam element with the first column corresponding to e1 and so on.

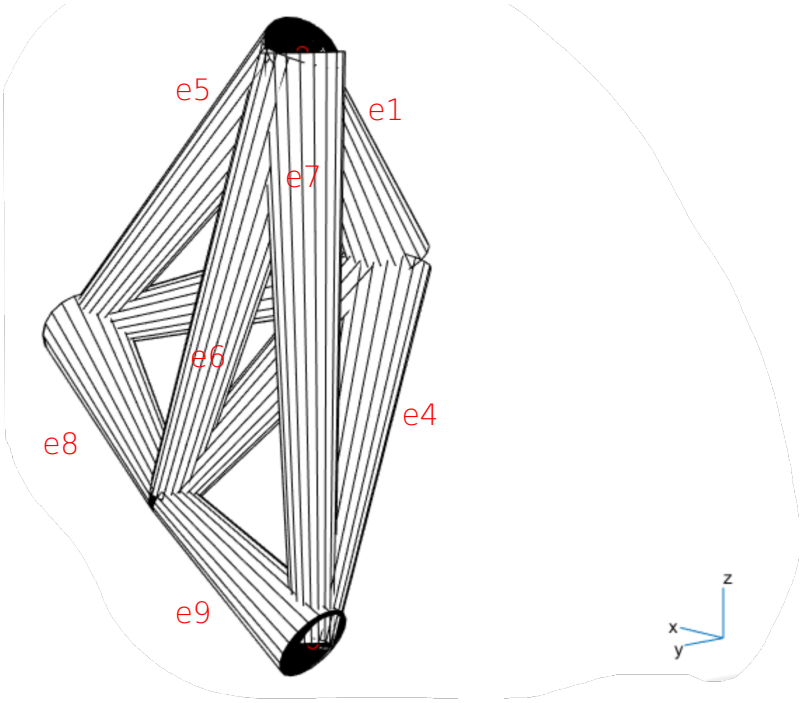

Figure 4.9: Element naming scheme in the frame structure.

4.2.1 Aligning Torque Stiffness

d_1 [mm]	40	50	40	40	40	40	40	40	20
d_2 [mm]	20	30	20	20	20	20	20	20	40

Table 4.2: Diameters d_1 and d_2 for aligning torque stiffness.

With manual tuning of the beam diameters, the aligning torque stiffness calculated with the mathematical model falls short by 17% when compared to the Finite Element model of the knuckle and has a mass of 3.45 [kg].

4.2.2 Camber Stiffness

d_1 [mm]	50	40	40	40	50	40	50	40	20
d_2 [mm]	20	20	20	20	20	18	30	20	40

Table 4.3: Diameters d_1 and d_2 for camber stiffness.

Similarly, with the manual optimization of the frame structure, the camber stiffness was found to be lesser by 22% when compared to the Finite Element model of the knuckle and has a mass of 3.83 [kg].

5

Conclusion

Based on the comprehensive results discussed in the previous chapter, we can confidently conclude that the frame structure developed using 3D beam elements by joining the outer hardpoints is a viable method for approximating the knuckle's stiffness and mass. This methodology has proven particularly effective for the camber and aligning torque stiffness of a rear knuckle, as thoroughly tested and validated in this thesis.

A significant aspect of this study is the manual iteration of the parameters, specifically the beam diameters (d_1 & d_2), to approximate the knuckle's stiffness and mass. Despite the manual process, the mathematical model demonstrated a strong correlation with the finite element model, maintaining an error margin within 25 percent when optimized manually. This level of accuracy, combined with the reduced complexity of the model, provides a practical tool for engineers in the early concept phases of suspension development.

5.1 Future Works

Although the results were within the expected range of deviation, the process of manually adjusting the beam diameters to meet various kinematic stiffness targets is inherently time-consuming and labor-intensive. Therefore, future work should focus on the development and implementation of a multi-objective optimization routine. Such a routine would automate the matching of both the mass and stiffness targets with the corresponding beam diameters, thereby enhancing efficiency.

Moreover, in the current study, the outer hardpoints were connected using a single linearly varying beam element. For future research, it would be beneficial to discretize this beam into several smaller beams. This discretization would afford greater control over the optimization process and is expected to yield even more accurate results. By breaking the beam into multiple segments, we could fine-tune the structural characteristics more precisely, potentially leading to improved performance metrics.

In conclusion, the methodology and findings presented in this thesis provide a solid foundation for further exploration and application. This framework can be extended to other components such as link arms, axles, and various structural elements.

Bibliography

[1] J. Knapczyk and S. Dzierz˙ek, "Displacement and force analysis of five-rod suspension with flexible joints," *Journal of Mechanical Design*, vol. 117, no. 4, pp. 532–538, Dec. 1995, ISSN: 1528-9001. DOI: 10.1115/1.2826715.

[2] A. Tena-Colunga, "Stiffness formulation for nonprismatic beam elements," *Journal of Structural Engineering*, vol. 122, no. 12, pp. 1484–1489, 1996. DOI: 10.1061/(ASCE)0733-9445(1996)122:12(1484).

[3] E. Rocca and R. Russo, "A feasibility study on elastokinematic parameter identification for a multilink suspension," *Proceedings of the Institution of Mechanical Engineers, Part D: Journal of Automobile Engineering*, vol. 216, no. 2, pp. 153–160, 2002. DOI: 10.1243/0954407021528995.

[4] G.-Y. Kim, S.-H. Han, and K.-H. Lee, "Structural optimization of a knuckle with consideration of stiffness and durability requirements," *The Scientific World Journal*, vol. 2014, pp. 1–7, 2014, ISSN: 1537-744X. DOI: 10.1155/2014/763692.

[5] D. G. Pavlou, "Chapter 7 - frames," in *Essentials of the Finite Element Method*, D. G. Pavlou, Ed., Academic Press, 2015, pp. 213–278, ISBN: 978-0-12-802386-0. DOI: https://doi.org/10.1016/B978-0-12-802386-0.00007-4.

[6] A. Nesterenko, G. Stolpovskiy, and M. Nesterenko, "Method of calculation flexural stiffness over natural oscillations frequencies," *Archives of Civil Engineering*, vol. 64, no. 4, pp. 89–103, Dec. 2018, ISSN: 1230-2945. DOI: 10.2478/ace-2018-0046.

[7] T. Abrahammson, "Structural dynamics and linear systems," in Chalmers University oif Technology, 2019, ch. 2.3.3. One Dimensional FE elements for trusses and frames.

[8] C. Iandiorio, D. Milani, and P. Salvini, "Shape optimization of 2d beam-structures to obtain the uniform strength," *IOP Conference Series: Materials Science and Engineering*, vol. 1275, no. 1, p. 012 030, Feb. 2023, ISSN: 1757-899X. DOI: 10.1088/1757-899x/1275/1/012030.

A

Appendix 1

This function computes the stiffness matrix for the system stiffness matrix, the transfer function for separate elements, and assembles.

Code Snippet A.1: The MATLAB function to formulate the global stiffness matrix

```
function K=Kmatrix(tot_dof,nel,ele_nodes,node_coor,E,G,d)

% Preallocation of the global stiffness matrix of the
   system
K=zeros(tot_dof);

% Loops over all the elements of the frame strucuture
for i=1:nel
    idx=ele_nodes(I,:);

    % Element node's respective degrees of freedom
    ele_dof=[6*idx(1)-5 6*idx(1)-4 6*idx(1)-3 ...
             6*idx(1)-2 6*idx(1)-1 6*idx(1)...
             6*idx(2)-5 6*idx(2)-4 6*idx(2)-3 ...
             6*idx(2)-2 6*idx(2)-1 6*idx(2)];

    % Node coordinates of the element
    x1=node_coor(idx(1),1); x2=node_coor(idx(2),1);
    y1=node_coor(idx(1),2); y2=node_coor(idx(2),2);
    z1=node_coor(idx(1),3); z2=node_coor(idx(2),3);

    % Length of the element
    L = sqrt((x2-x1)^2 + (y2-y1)^2 + (z2-z1)^2);

    % Stiffness Matrix Formulation for continuously
       varying circular 3D beam

    % Closed-form solutions to flexibility terms for
       linearly tapered circular members
```

```
f11 = (((4*L)/(pi*E*d(i,1)^2)) * (d(i,1)/(d(i,2)-d(i
   ,1))) * (1-(d(i,1)/d(i,2))));

f22 = ((((64*L^3)/(3*pi*E*d(i,1)^4))*(d(i,1)/d(i,2))
   ^3) + (((40*L)/(9*pi*G*d(i,1)^2))*(d(i,1)/(d(i,2)-
   d(i,1)))*(1-(d(i,1)/d(i,2)))));

f33=f22;

f26 = (((64*L^2)/(3*pi*E*d(i,1)^4))*((d(i,1)/d(i,2))
   ^3 + (0.5*((d(i,1)/(d(i,2)-d(i,1)))^2) * (1 + ((d(
   i,1)/d(i,2))^2) - (2*d(i,1)/d(i,2))))));

f35=f26;

f66 = (((64*L)/(3*pi*E*d(i,1)^4))*(d(i,1)/(d(i,2)-d(i
   ,1)))*(1-(d(i,1)/d(i,2))^3));

f55=f66;

f44 = (((32*L)/(3*pi*G*d(i,1)^4))*(d(i,1)/(d(i,2)-d(i
   ,1)))*(1-(d(i,1)/d(i,2))^3));

% Stiffness coefficients
% Axial and torsional stiffness coefficients
rax = 1/f11;
rj = 1/f44;

% Major bending-stiffness coefficients
detx = f22*f66 - f26^2;
r11x = f22/detx;
r12x = (f26*L - f22)/detx;
r22x = (f66*L^2 - 2*f26*L + f22)/detx;
raax = (r11x+r22x+2*r12x)/L^2;
rabx = (r11x+r12x)/L;
rbax = (r22x+r12x)/L;

% Minor bending-stiffness coefficients
dety = f33*f55 - f35^2;
r11y = f33/dety;
r12y = (f35*L-f33)/dety;
r22y = (f55*L^2-2*f35*L+f33)/dety;
raay = (r11y+r22y+2*r12y)/L^2;
raby = (r11y+r12y)/L;
rbay = (r22y+r12y)/L;
```

```
    % Stiffness matrix formation
    k11 = diag([rax,raax,raay,rj,r11y,r11x]);
    k11(2,6) = rabx; k11(3,5) = -raby;
    k11(6,2) = rabx; k11(5,3) = -raby;

    k22 = diag([rax,raax,raay,rj,r22y,r22x]);
    k22(2,6) = -rbax; k22(3,5) = rbay;
    k22(6,2) = -rbax; k22(5,3) = rbay;

    k12 = diag([-rax,-raax,-raay,-rj,r12y,r12x]);
    k12(2,6) = rbax; k12(3,5) = -rbay;
    k12(6,2) = -rabx; k12(5,3) = raby;

    k21 = k12';

    % Local stiffness matrix
    k = [k11 k12; k21 k22];

    if x1 == x2 && y1 == y2
        if z2 > z1
            R = [0 0 1; 0 1 0; -1 0 0];
        else
            R = [0 0 -1; 0 1 0 ;1 0 0];
        end
    else
        CXx = (x2-x1)/L; CYx = (y2-y1)/L; CZx = (z2-z1)/L
           ;
        D = sqrt(CXx^2 + CYx^2);
        CXy = -CYx/D; CYy = CXx/D; CZy = 0;
        CXz = -CXx*CZx/D; CYz = -CYx*CZx/D; CZz = D;

        % Rotation Matrix
        R = [CXx CYx CZx ;CXy CYy CZy ;CXz CYz CZz];
    end

    % Transformation Matrix
    T = [R zeros(3,9); zeros(3) R zeros(3,6);
        zeros(3,6) R zeros(3); zeros(3,9) R];

    % Global stiffness matrix
    K(ele_dof,ele_dof) = K(ele_dof,ele_dof)+T.'*k*T;
end
```

DEPARTMENT OF SOME SUBJECT OR TECHNOLOGY
CHALMERS UNIVERSITY OF TECHNOLOGY
Gothenburg, Sweden
www.chalmers.se

CHALMERS
UNIVERSITY OF TECHNOLOGY